

Discussion on “Pseudo-Mach angles for Rayleigh ground waves generated by trains moving at conventional speeds [J. Sound Vib. 570 (2024) 118121]”

van Dalen, Karel N.

DOI

[10.1016/j.jsv.2024.118586](https://doi.org/10.1016/j.jsv.2024.118586)

Publication date

2024

Document Version

Final published version

Published in

Journal of Sound and Vibration

Citation (APA)

van Dalen, K. N. (2024). Discussion on “Pseudo-Mach angles for Rayleigh ground waves generated by trains moving at conventional speeds [J. Sound Vib. 570 (2024) 118121]”. *Journal of Sound and Vibration*, 590, Article 118586. <https://doi.org/10.1016/j.jsv.2024.118586>

Important note

To cite this publication, please use the final published version (if applicable). Please check the document version above.

Copyright

Other than for strictly personal use, it is not permitted to download, forward or distribute the text or part of it, without the consent of the author(s) and/or copyright holder(s), unless the work is under an open content license such as Creative Commons.

Takedown policy

Please contact us and provide details if you believe this document breaches copyrights. We will remove access to the work immediately and investigate your claim.

Green Open Access added to TU Delft Institutional Repository

'You share, we take care!' - Taverne project

<https://www.openaccess.nl/en/you-share-we-take-care>

Otherwise as indicated in the copyright section: the publisher is the copyright holder of this work and the author uses the Dutch legislation to make this work public.

Contents lists available at [ScienceDirect](https://www.sciencedirect.com)

Journal of Sound and Vibration

journal homepage: www.elsevier.com/locate/jsvi

Discussion on “Pseudo-Mach angles for Rayleigh ground waves generated by trains moving at conventional speeds [J. Sound Vib. 570 (2024) 118121]”

Karel N. van Dalen

TU Delft, Faculty of Civil Engineering and Geosciences, Department of Engineering Structures, Section of Dynamics of Solids & Structures, Stevinweg 1, 2628 CN Delft, the Netherlands

ARTICLE INFO

Keywords

Moving load
Sub-Rayleigh velocity
Plane Rayleigh waves
Frequency-dependent radiation angle
Mechanism of generation

1. Introduction

The paper of Krylov [1] demonstrates that radiation of plane Rayleigh waves excited by a constant load moving on a beam with discrete, periodic supports that rest on an elastic half-space can take place at speeds of the moving load smaller than the Rayleigh-wave velocity and at angles that are different from the conventional Mach angle. This discussion paper presents an expression for the frequency-dependent radiation angle as well as conditions for the existence of the plane Rayleigh waves, it further clarifies the mechanism of the radiation of the waves, and it demonstrates their physical significance. First, an alternative closed-form representation for the response in the space-frequency domain is presented to reveal expressions for the wavenumbers in horizontal directions (and thus for the angles of the radiated waves) as well as the conditions for existence based on those. Then, by comparing with the wave field excited in the canonical case of an harmonically varying load moving directly on the surface of the half-space (at sub-Rayleigh velocity), it is found that the basic mechanism of plane-wave generation is not fundamentally different. In both cases, the plane Rayleigh waves are radiated due to the time-periodic nature of the loading moving/progressing on the half-space surface. More specifically, all harmonic components representing the set of sequentially exerted sleeper forces continuously radiate Rayleigh waves leading to the occurrence of plane waves, just like the harmonic load moving directly on the half-space surface creates them. It is therefore claimed that the plane Rayleigh waves demonstrated in [1] are not unconventional; they are simply the elementary components of the well-known curved Rayleigh-wave pattern excited by the harmonic load moving directly on the half-space surface, as well as of the very similar Rayleigh-wave pattern excited by the set of sleeper forces. The radiated plane waves do not add up to the classical Mach cone – which is indeed due to the frequency dependence of the radiation angle [1] – but together constitute the curved wave patterns. The destructive interference of the plane Rayleigh waves is therefore only partial and their physical significance is evident.

E-mail address: K.N.vanDalen@tudelft.nl.

<https://doi.org/10.1016/j.jsv.2024.118586>

Received 20 December 2023; Received in revised form 3 June 2024; Accepted 7 June 2024

Available online 8 June 2024

0022-460X/© 2024 Elsevier Ltd. All rights are reserved, including those for text and data mining, AI training, and similar technologies.

2. Radiation angles and conditions for existence of the plane Rayleigh waves

To arrive at the alternative expression for the space-frequency domain response (to that shown in Eq. (A.6) of [1]), we first rewrite the space-frequency domain expression for the loading on the half-space (i.e., the set of forces sequentially exerted by the sleepers, Eq. (A.5) of [1]) using the Fourier series representation of a Dirac comb (for later reference, the time-domain expression for the loading is also given here):

$$\begin{aligned}\hat{p}(x, y, \omega) &= \hat{p}(\omega)\delta(y)e^{i\frac{\omega}{v}x} \sum_{n=-\infty}^{\infty} \delta(x - nd) = \hat{p}(\omega)\delta(y) \frac{1}{d} \sum_{n=-\infty}^{\infty} e^{i\frac{\omega - \omega_n}{v}x}, \quad \omega_n = n \frac{2\pi v}{d}, \\ p(x, y, t) &= P(t - x/v)\delta(y) \sum_{n=-\infty}^{\infty} \delta(x - nd) = P(t - x/v)\delta(y) \frac{1}{d} \sum_{n=-\infty}^{\infty} e^{-i\frac{\omega_n}{v}x}.\end{aligned}\quad (1)$$

Here, x and y denote the longitudinal and transversal horizontal coordinates, respectively, t denotes time, ω the angular frequency, while v denotes the vehicle velocity and d the sleeper spacing; i is the imaginary unit. Furthermore, $\hat{P}(\omega)$ denotes the Fourier transform of the force $P(t)$ exerted by the sleeper support at $x = 0$, and ω_n denotes the sleeper passing frequency together with its integer multiples ($|n| > 1$). Contrary to the notation in [1], the symbol p (lower case) is used in the left-hand side of Eq. (1) to discriminate it from P (capital) in the right-hand side, as the quantities have slightly different physical meaning; in addition, the hat symbol is used in the current paper to indicate that the quantity belongs to the frequency domain. Finally, we note that $\omega \geq 0$ is considered throughout the paper, which is sufficient for real-valued time-domain signals.

The response of the half-space to the loading can be derived by applying the Fourier transform over x and y , solving the transformed elastodynamic equations of motion (i.e., a set of ordinary differential equations that only depend on the vertical coordinate z) accounting for the boundary conditions at the surface as well as for the radiation condition, and subsequently evaluating the inverse Fourier integrals (the boundary conditions at $z = 0$ are zero shear stresses and non-zero normal stress; the latter is equal to minus the loading specified in Eq. (1)). This is a well-known method detailed in many textbooks [e.g., 2–5], and therefore only the main steps are shown here for brevity. For simplicity, we assume material damping to be absent.

When Fourier-transformed over x and y , the expression for the loading (Eq. (1)) reads as follows (the tilde indicates that the quantity lives in the frequency-wavenumber (ω, k_x, k_y) domain):

$$\tilde{p}(k_x, k_y, \omega) = 2\pi \frac{\hat{P}(\omega)}{d} \sum_{n=-\infty}^{\infty} \delta(k_x - k_{x,n}), \quad k_{x,n} = \frac{\omega - \omega_n}{v}. \quad (2)$$

The following frequency-wavenumber domain representation for the particle velocity at the surface of the half-space can be obtained:

$$\tilde{v}_z(k_x, k_y, z=0, \omega) = 2\pi \frac{i\omega \hat{P}(\omega) k_s^2}{Gd} \frac{q_p}{F(k)} \sum_{n=-\infty}^{\infty} \delta(k_x - k_{x,n}), \quad (3)$$

where $F(k)$ denotes the Rayleigh determinant (see [1]), $k^2 = k_x^2 + k_y^2$ and $q_p = \sqrt{k^2 - k_p^2}$, k_p and k_s denote the wavenumbers of the compressional and shear waves, respectively, and G the shear modulus of the half-space. The inverse Fourier integral over k_x can be evaluated employing the shifting property of the Dirac delta function, and the inverse Fourier integral over k_y can be evaluated subsequently using Cauchy's residue theorem. For $y > 0$, this entails

$$\begin{aligned}\hat{v}_z(x, y, z=0, \omega) &= \frac{1}{4\pi^2} \int_{-\infty}^{\infty} \int_{-\infty}^{\infty} \tilde{v}_z(k_x, k_y, z=0, \omega) e^{i(k_x x + k_y y)} dk_x dk_y \\ &= \frac{1}{2\pi} \frac{i\omega \hat{P}(\omega) k_s^2}{Gd} \sum_{n=-\infty}^{\infty} \int_{-\infty}^{\infty} \frac{q_p}{F(k)} \Big|_{k_x=k_{x,n}} e^{i(k_{x,n} x + k_y y)} dk_y \\ &\approx -\frac{\omega \hat{P}(\omega) k_s^2 k_R q_p(k_R)}{Gd \, dF/dk|_{k=k_R}} \sum_{n=-\infty}^{\infty} \frac{1}{k_{y,n}} e^{i(k_{x,n} x + k_{y,n} y)},\end{aligned}\quad (4)$$

where $dF/dk|_{k=k_R} = dF/dk|_{k_x=k_{x,n}, k_y=k_{y,n}}$ (note that $k_{x,n}$ and $k_{y,n}$ combine to the Rayleigh wavenumber k_R in $F(k)$ and in q_p), and

$$k_{y,n} = \begin{cases} \sqrt{k_R^2 - k_{x,n}^2}, & k_R^2 > k_{x,n}^2, \\ i\sqrt{k_{x,n}^2 - k_R^2}, & k_R^2 < k_{x,n}^2. \end{cases} \quad (5)$$

Note that, in full correspondence with the analysis in [1], only the Rayleigh-pole contribution has been taken into account in the evaluation of the inverse Fourier integral over k_y (it dominates the response far from the source); the contributions of the loop integrals along the branch cuts, yielding compressional and shear waves [e.g., 3,6], have been ignored.

The alternative expression for the frequency-domain response (Eq. (4)) has been obtained using double Fourier transformation. This method is somewhat different from that employed in [1]. To show that the same result can be obtained with that method, in Appendix A we evaluate the convolution of the modified expression for the loading (Eq. (1)) with the Green's function of the half-space in an approximate manner; the result in Eq. (A.3) confirms Eq. (4), but it is only valid for real-valued $k_{y,n}$, and we therefore base our interpretation on Eq. (4).

The latter expression clearly shows that the frequency-domain response contains plane Rayleigh waves that propagate away from the track (in positive y direction) for $k_{y,n} > 0$. If $k_{y,n}$ is imaginary (i.e., for $k_R^2 < k_{x,n}^2$), the frequency-domain response does not consist of propagating plane waves but of waves that are evanescent in y direction. This confirms the numerical findings presented in [1], although these were not related to the nature of $k_{y,n}$. It also confirms the following observations made from Fig. 2, 3 and 5 of [1], respectively:

- For $\omega > \omega_n$, the phase propagation is in positive x direction as $k_{x,n} > 0$.
- For $\omega < \omega_n$, the phase propagation is in negative x direction as $k_{x,n} < 0$.
- For $\omega = \omega_n$, there is no phase propagation in x direction as $k_{x,n} = 0$.

However, Eq. (4) also reveals the following aspects:

- The direction of propagation of the plane waves is defined by the radiation angle $\theta_n = \theta_n(\omega) = \arctan(k_{y,n}/k_{x,n})$ (measured from the positive x axis), which is indeed frequency (ω) dependent.
- The bounds of the frequency bands around ω_n in which the radiation of plane Rayleigh waves takes place can be determined from the fact that $k_{y,n}$ should be real-valued, leading to

$$\begin{aligned} \omega_n \frac{c_R}{c_R + v} < \omega < \omega_n \frac{c_R}{c_R - v}, & \text{ for } \omega_n > 0, \\ \omega_n \frac{c_R}{c_R - v} < \omega < \omega_n \frac{c_R}{c_R + v}, & \text{ for } \omega_n < 0, \end{aligned} \quad (6)$$

where c_R denotes the Rayleigh-wave speed. The first condition essentially explains why in Fig. 4 of [1] the plane Rayleigh waves are not observed. The second condition states that Eq. (4) yields plane Rayleigh waves for a range of negative frequencies. As mentioned earlier, negative frequencies are not considered, and the second condition can therefore be ignored.

3. Mechanism of plane-Rayleigh wave generation

To further clarify the mechanism of plane Rayleigh-wave generation, we consider an harmonic load moving directly on the half-space surface at sub-Rayleigh velocity, with oscillation frequency being the sleeper passing frequency (it could also be a multiple of that):

$$\begin{aligned} \hat{p}(x, y, \omega) &= \delta(y) \sum_{n=-1,1} \frac{P_n}{v} e^{i \frac{\omega - \omega_n}{v} x}, \\ p(x, y, t) &= 2P_1 \delta(x - vt) \delta(y) \cos(\omega_1 x/v) = \delta(x - vt) \delta(y) \sum_{n=-1,1} P_n e^{-i \frac{\omega_n}{v} x}, \end{aligned} \quad (7)$$

where $P_1 = P_{-1}$ denotes half of the force amplitude; note that the $\cos(\omega_1 x/v)$ in the expression for $p(x, y, t)$ could be replaced by $\cos(\omega_1 t)$, but the former facilitates the comparison (below) with the loading composed of the set of sleeper forces. The frequency-domain response associated with Eq. (7) can be derived in the same manner as in Section 2. The result reads

$$\hat{v}_z(x, y, z=0, \omega) \approx -\frac{\omega k_s^2 k_R q_p(k_R)}{Gv \, dF/dk|_{k=k_R}} \sum_{n=-1,1} \frac{P_n}{k_{y,n}} e^{i(k_{x,n}x + k_{y,n}y)}, \quad (8)$$

where the wavenumbers $k_{x,n}$ and $k_{y,n}$ are defined in exactly the same manner as before (Eqs. (2) and (5), respectively), and so is $dF/dk|_{k=k_R}$.

Comparing Eq. (8) with Eq. (4), the resemblance is obvious. Clearly, the harmonically varying moving load also radiates plane Rayleigh waves in a specific frequency band (i.e., only in the frequency band around the sleeper passing frequency), while it creates evanescent waves outside. As compared to the response of the half-space to the set of sleeper forces (Eq. (4)), the same conclusions can be drawn regarding the direction of phase propagation in x direction, the frequency-dependent angle of radiation, and the frequency band of existence. This is actually not a surprise given the similarity of the loadings in both the frequency and time domains, see Eqs. (1) and (7) (the latter consists of only one harmonic while the former consists of infinitely many). Hence, we conclude that the mechanism of plane Rayleigh-wave generation by a *constant* load moving at sub-Rayleigh velocity on a beam with discrete, periodic supports that rest on an elastic half-space is not fundamentally different from that in the canonical case of a *harmonic* load moving (also at sub-Rayleigh velocity) directly on the half-space surface. In both cases, the plane Rayleigh waves are radiated due to the time-periodic nature of the loading moving/progressing on the half-space surface. More specifically, all harmonic components

representing the set of sleeper forces (Eq. (1)) continuously radiate Rayleigh waves (in their own frequency bands) leading to the occurrence of plane waves, just like the harmonic load moving directly on the half-space surface creates them (in a single frequency band). Hence, it is claimed that the plane Rayleigh waves demonstrated in [1] are not unconventional.

It should be noted, however, that even if infinitely many harmonic components are taken into account for the load that moves directly on the half-space surface (i.e., that loading will be periodic in time, not harmonic),

$$\hat{p}(x, y, \omega) = \delta(y) \sum_{n=-\infty}^{\infty} \frac{P_n}{v} e^{-\frac{\omega - \omega_n}{v} x}, \quad p(x, y, t) = \delta(x - vt) \delta(y) \sum_{n=-\infty}^{\infty} P_n e^{-\frac{\omega_n}{v} x}, \quad (9)$$

with $P_{-n} = P_n$, the response will not be exactly the same as that induced by the set of sleeper forces, because the energy distribution over the frequencies is different. This is clear from the difference in $\hat{P}(\omega)$ and P_n in Eqs. (1) and (9), respectively, and implies different weights of the various wavenumbers $k_{x,n}$ and $k_{y,n}$ which depend on frequency, and thus of the plane Rayleigh waves radiated in various directions; the difference in weights can already be observed from the comparison of Eqs. (4) and (8) (see also Section 4 for an illustration). Related to that, the periodic load moving directly on the half-space surface is only present for infinitesimally short duration at a single location, while the forces exerted by the sleepers generally have a finite duration. The loadings are exactly same only if $\hat{P}(\omega) = P_1 d / v$ and $P_n = P_1$, leading to (compare Eqs. (1) and (9))

$$\begin{aligned} \hat{p}(x, y, \omega) &= \frac{P_1}{v} \delta(y) \sum_{n=-\infty}^{\infty} e^{-\frac{\omega - \omega_n}{v} x}, \\ p(x, y, t) &= P_1 \delta(x - vt) \delta(y) \sum_{n=-\infty}^{\infty} e^{-\frac{\omega_n}{v} x} = P_1 d \delta(x - vt) \delta(y) \sum_{n=-\infty}^{\infty} \delta(x - nd). \end{aligned} \quad (10)$$

In that case, both loadings consists of the same infinitely short Dirac pulses at the sleeper locations (note the difference between $P(t - x/v)$ and $\delta(x - vt) \sim \delta(t - x/v)$ in Eqs. (1) and (10)), and the energy distributions over the different frequencies/plane Rayleigh waves are therefore exactly the same.

4. Physical significance of the radiated plane Rayleigh waves

Ref. [1] states that “in contrast to the conventional Mach angles, values of pseudo-Mach angles do depend on frequency, which means that waves radiated at different frequency components will propagate at different angles, causing the destructive interference that would suppress radiated plane waves”. To verify this statement, Fig. 1 presents snapshots of the space-time domain Rayleigh-wave field induced by the set of sleeper forces as well as that induced by the harmonic load moving directly on the half-space surface; for reasons of comparison, only the first harmonic has been taken into account for the former (i.e., $n = 1$ and $n = -1$). The responses were obtained by numerical evaluation of the inverse Fourier transform of Eqs. (4) and (8), respectively (the integrable singularities were handled analytically).

Starting with the response to the harmonic load moving directly on the half-space surface as shown in Fig. 1a, it is noted that the radiated plane waves are simply the elementary components of the generated well-known Rayleigh-wave pattern (it can be verified that this pattern is symmetric with respect to the path of the moving load). The plane waves, radiated in different directions, together constitute the curved wave pattern. As for the response induced by the set of sleeper forces (Fig. 1b), which is a very similar, the radiated plane waves are simply the elementary components of that generated Rayleigh-wave pattern too. Hence, the physical

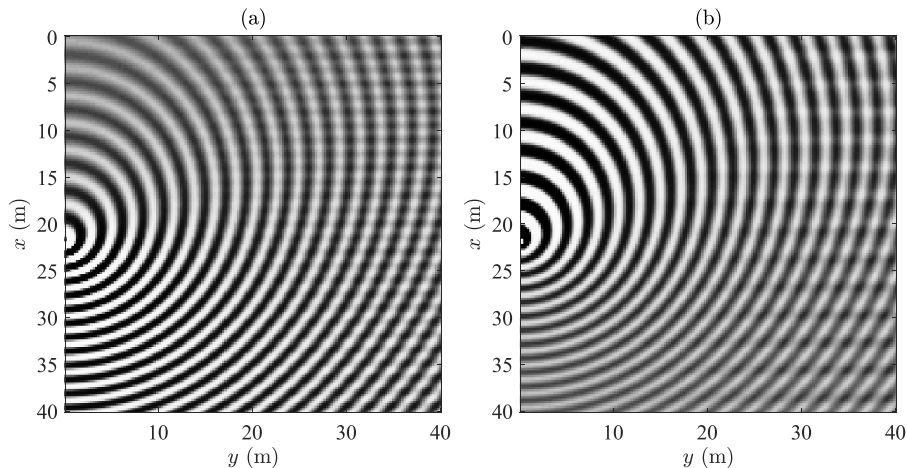


Fig. 1. Snapshots of the Rayleigh-wave field (vertical particle velocity) induced by the harmonic load moving directly on the half-space surface (panel a) and induced by the set of sleeper forces (only the contributions of $n = 1$ and $n = -1$; panel b). The load position is: $x \approx 22$ m, $y = 0$.

significance of the plane waves described in [1] is evident and their destructive interference is only partial. On the other hand, Fig. 1 confirms that the radiated plane waves do not add up to the classical Mach cone, which is indeed due to the frequency dependence of the radiation angle (which was specified in Section 2).

When comparing the responses shown in Fig. 1, it is confirmed (see Section 3) that the energy distribution over directions in the generated Rayleigh-wave fields is different as the various plane waves have different weights. In Fig. 1a, the magnitude of the field radiated in forward direction is largest, while the magnitude of the backward radiated field is largest in Fig. 1b. The latter is due to the decay of $\widehat{P}(\omega)$ with increasing ω [1], which suppresses the higher frequencies in the band of propagating waves around ω_1 , and thus the waves radiated in forward direction relative to the backward-radiated ones.

The complete response induced by the set of sleeper forces obviously includes the response to a static load ($n = 0$) as well as to the higher harmonics ($|n| > 1$). One can verify that the latter give rise to similar wave patterns as shown in Fig. 1b but have shorter wave lengths. However, these short wave-length contributions are not necessarily energetic; the frequencies in the bands around higher ω_n are suppressed due to the above-mentioned decay of $\widehat{P}(\omega)$.

5. Conclusions

This discussion paper presented an alternative closed-form representation (to that shown in Eq. (A.6) of [1]) for the space-frequency domain response of the half-space surface to reveal expressions for the radiation angle of the plane Rayleigh waves excited by the set of sequentially exerted sleeper forces as well as conditions for existence of the waves. Furthermore, by comparing with the wave field excited in the canonical case of a harmonically varying load moving directly on the surface of the half-space, it was found that the basic mechanism of plane-wave generation is not fundamentally different. All harmonic components representing the set of sleeper forces continuously radiate Rayleigh waves leading to the occurrence of plane waves, just like the harmonic load moving directly on the half-space surface creates them. It is therefore claimed that the plane Rayleigh waves demonstrated in [1] are not unconventional; they are simply the elementary components of the well-known curved Rayleigh-wave pattern excited by the harmonic load moving directly on the half-space surface, as well as of the very similar Rayleigh-wave pattern excited by the set of sleeper forces.

CRedit authorship contribution statement

Karel N. van Dalen: Writing – review & editing, Writing – original draft, Methodology, Investigation, Formal analysis.

Declaration of competing interest

The authors declare that they have no known competing financial interests or personal relationships that could have appeared to influence the work reported in this paper.

Data availability

Data will be made available on request.

Appendix A

Eq. (4) presented the alternative expression (to that shown in Eq. (A.6) of [1]) for the frequency-domain response obtained using double Fourier transformation. To show that the same result can be obtained with the method employed in [1], we here derive an approximation of the convolution integral of the modified expression for the loading (Eq. (1)) with the Green's function G_{zz} of the half-space (i.e., the Rayleigh-wave contribution to the Green's function, which is Eq. (A.2) of [1]).

To this end, we can write (see also Eq. (A.1) of [1]) the following for $y > 0$:

$$\begin{aligned} \widehat{v}_z(x, y, z = 0, \omega) &= \int_{-\infty}^{\infty} \int_{-\infty}^{\infty} p(x', y', \omega) G_{zz}(x - x', y - y', \omega) dx' dy' \\ &= \frac{\widehat{P}(\omega)}{d} \sum_{n=-\infty}^{\infty} \int_{-\infty}^{\infty} e^{ik_{x,n}x'} G_{zz}(x - x', y, \omega) dx' = \frac{\widehat{P}(\omega)D(\omega)}{d} \sum_{n=-\infty}^{\infty} \int_{-\infty}^{\infty} \frac{e^{i\varphi(x')y}}{\sqrt{r(x')y}} dx', \end{aligned} \quad (\text{A.1})$$

where

$$\varphi(x') = k_{x,n} \frac{x'}{y} + k_R r(x'), \quad r(x') = \sqrt{1 + \frac{(x - x')^2}{y^2}}. \quad (\text{A.2})$$

The integral over x' in Eq. (A.1) can be approximated using the method of stationary phase [5]. The result reads, for y being large and

positive, as follows:

$$\widehat{v}_z(x, y, z=0, \omega) \approx \frac{\sqrt{2\pi k_R} \widehat{P}(\omega) D(\omega)}{d} e^{i\frac{\pi}{4}} \sum_{n=-\infty}^{\infty} \frac{1}{k_{y,n}} e^{i(k_{x,n}x + k_{y,n}y)}, \quad (\text{A.3})$$

where we used (x'_s) denotes the stationary point; $k_{x,n}$ and $k_{y,n}$ have been defined in Section 2)

$$x'_s = x - \frac{k_{x,n}}{k_{y,n}}y, \quad r(x'_s) = \frac{k_R}{k_{y,n}}, \quad \varphi(x'_s) = k_{x,n}\frac{x}{y} + k_{y,n}, \quad \left. \frac{\partial^2 \varphi}{\partial x'^2} \right|_{x'=x'_s} = \frac{k_{y,n}k_{y,n}^2}{k_R^2 y^2}. \quad (\text{A.4})$$

Using the expression for $D(\omega)$ taken from [1], it can easily be verified that Eq. (A.3) is identical to Eq. (4), which confirms that result. However, strictly speaking, the result in Eq. (A.3) is only valid for real-valued $k_{y,n}$, in other words for $k_R^2 > k_{x,n}^2$; otherwise, the stationary point becomes complex and does no longer lie on the x' path of integration (see Eq. (A.1)). Hence, Eq. (A.3) only confirms the propagating-wave parts of Eq. (4), not the evanescent-wave parts. In relation to that, the different components (n) of Eq. (A.3) in fact have different frequency (ω) ranges of validity.

References

- [1] V.V. Krylov, Pseudo-Mach angles for Rayleigh ground waves generated by trains moving at conventional speeds, *J. Sound Vib.* 570 (2024) 118121, <https://doi.org/10.1016/j.jsv.2023.118121>.
- [2] J.D. Achenbach, *Wave Propagation in Elastic Solids*, North-Holland Publishing Company, Amsterdam, New York, 1973.
- [3] W. Ewing, W. Jardetsky, F. Press, *Elastic Waves in Layered Media*, McGraw-Hill Book Company, New York, Toronto, London, 1957.
- [4] L. Frýba, *Vibration of Solids and Structures Under Moving Loads*, Noordhoff International Publishing, Groningen, 1973.
- [5] J. Miklowitz, *The Theory of Elastic Waves and Waveguides*, North-Holland Publishing Company, Amsterdam, New York, Oxford, 1987.
- [6] K.N. van Dalen, G.G. Drijkoningen, D.M.J. Smeulders, Pseudo interface waves observed at the fluid/porous-medium interface: a comparison of two methods, *J. Acoust. Soc. Am.* 129 (2011) 2912–2922, <https://doi.org/10.1121/1.3557040>.